6

Power Fluctuations in a Wind Farm Compared to a Single Turbine

Joaquin Mur-Amada and Jesús Sallán-Arasanz
Zaragoza University
Spain

1. Introduction

This chapter is focused on the estimation of wind farm power fluctuations from the behaviour of a single turbine during continuous operation (special events such as turbine tripping, grid transients, sudden voltages changes, etc. are not considered). The time scope ranges from seconds to some minutes and the geographic scope is bounded to one or a few nearby wind farms.

One of the objectives of this chapter is to explain quantitatively the wind power variability in a farm from the behaviour of a single turbine. For short intervals and inside a wind farm, the model is based on the experience with a logger system designed and installed in four wind farms (Sanz et al., 2000a), the classic theory of Gaussian (normal) stochastic processes, the wind coherence model (Schlez & Infield, 1998), and the general coherence function derived by Risø Institute in Horns Rev wind farm (Martins et al., 2006; Sørensen et al., 2008a). For larger distances and slower variations, the model has been tested with meteorological data from the weather network.

The complexities inherent to stochastic processes are partially circumvented presenting some case studies with meaningful graphs and using classical tools of signal processing and time series analysis when possible. The sum of the power from many turbines is a stochastic process that is the outcome of many interactions from different sources. The sum of the power variations from more than four turbines converges approximately to a Gaussian process despite of the process nature (deterministic, stochastic, broadband or narrowband), analogously to the martingale central limit theorem (Hall & Heyde, 1980). The only required condition is the negligible effect of synchronization forces among turbine oscillations.

The data logged at some wind farms are smooth and they have good mathematical properties except during special events such as turbine breaker trips or severe weather. This chapter will show that, under some circumstances, the power output of a wind farm can be approximated to a Gaussian process and its auto spectrum density can be estimated from the spectrum of a turbine, wind farm dimensions and wind coherence. The wind farm power variability is fully characterized by its auto spectrum provided the Gaussian approximation is accurate enough. Many interesting properties such as the mean power fluctuation shape during a period, the distribution of power variation in a time period, the more extreme power variation expected during a short period, etc. can be estimated applying the outstanding properties of Gaussian processes according to (Bierbooms, 2008) and (Mur-Amada, 2009).

Since the canonical representation of a Gaussian stochastic process is its frequency spectrum (Karhunen–Loeve theorem), the analysis of wind power fluctuations is usually done in the frequency domain for convenience. An alternative to Fourier analysis is time series analysis. Time series are quite popular in stochastic models since they are well suited to prediction and their parameters and their properties can be easily estimated (Wangdee & Billinton, 2006). Even though the two mathematical techniques are quite related, the study of periodic behaviour is more direct through Fourier approach whereas the time series approach is more appropriate for the study of non-systematic behaviour.

1.1 Sources of wind power fluctuation

The fluctuations observed at the output of a turbine are the outcome of the interaction of wind turbulence with the complex turbine dynamics. For very slow fluctuations (corresponding to lower frequencies in the spectrum), the turbine regulation achieves its target and the turbine dynamics are negligible. Faster fluctuations (corresponding to higher frequencies) interact with the structural and drive-train vibrations. The complexity of the mechanical vibrations, the turbine control and the non-linearity of the generator power electronics interactions affects notably the generator electromagnetic torque and the turbine power fluctuations, especially in the frequency range from tenths of Hertzs to grid frequency.

There are many dynamic turbine models described in the literature. Most megawatt turbines share the following behaviour, considering the aerodynamic torque as the system input and the power injected in the grid as the system output (Soens, 2005; Comech-Moreno, 2007; Bianchi et al, 2006):

- Between cut-in and rated wind speeds, the turbine power usually behaves (with respect to the wind measured with an anemometer) as a low frequency first-order filter with a time constant between 1 and 10 s.
- Between rated and cut-out wind speeds, the turbine power usually behaves (with respect to the measured wind) as an asymmetric band pass filter of characteristic frequency around 0,3 Hz due to the combined effect of the slow action of the pitch/ active stall and the quicker speed controllers.
- At some characteristic frequencies, the turbine mechanical vibrations, the power electronics and the generator dynamics modify the general trend of the power output spectrum with respect to the wind input.

There are many specific characteristics that impact notably the power fluctuations and their realistic reproduction requires a comprehensive model of each turbine. The details of the control, the structural details and the power electronics implemented in the turbines are proprietary and they are not publicity available. In contrast, the electrical power injected by a turbine can be measured easily.

Moreover, some fluctuations in power are not proportional to the fluctuations in wind or aerodynamic torque. Thus, the ratio of the output signal divided by the input signal in the frequency domain is not constant. However, a statistical linear model in the frequency can be used (Welfonder et al., 1997) although the system output is neither proportional to the input nor deterministic.

The approach taken in this chapter is primarily phenomenological: the power fluctuations during the continuous operation of the turbines are measured and characterized for timescales in the range of minutes to fractions of seconds. Thus, one contribution of this

chapter is the experimental characterization of the power fluctuations of three commercial turbines. Some experimental measurements in the joint time-frequency domain are presented to test the mathematical model of the fluctuations and the variability of PSD is studied through spectrograms.
Other contribution of this chapter is the admittance of the wind farm: the oscillations from a wind farm are compared to the fluctuations from a single turbine, representative of the operation of the turbines in the farm. The partial cancellation of power fluctuations in a wind farm is estimated from the ratio of the farm fluctuation relative to the fluctuation of one representative turbine. Some stochastic models are derived in the frequency domain to link the overall behaviour of a large number of wind turbines from the operation of a single turbine.
This chapter is based mostly on the experience obtained designing, programming, assembling and analyzing two multipurpose measuring system installed in several wind farms (Sanz et at., 2000a; Mur-Amada, 2009). This measuring system has been the first prototype of a multipurpose data logger, now called AIRE (Analizador Integral de Recursos Energéticos), that is currently commercialized by Inycom and CIRCE Foundation.

1.2 Random and almost cyclic fluctuations

Power output fluctuations can be divided into almost cyclic components (tower shadow, wind shear, modal vibrations, etc.), wind farm weather dynamics (turbulence, boundary layer atmospheric stability, micrometeorological dynamics, etc.) and events (connection or disconnection of the turbine, change in generator configuration, etc.). The customary treatment of these fluctuations is done through Fourier transform.
Cyclic fluctuations due to tower shadow, wind shear, etc. present more systematic behaviour than weather related variations. Almost cyclic fluctuations are approximately periodic and they present quite definite frequencies. In this context, almost periodic means that the signal can be decomposed into a set of sinusoidal components with slow varying amplitudes (some of them non-harmonically related) and stationary noise (i.e., polycyclostationary signals). The frequencies in the signal vary slightly since the fluctuation amplitudes are not constant and the signal is not periodic in the conventional sense.

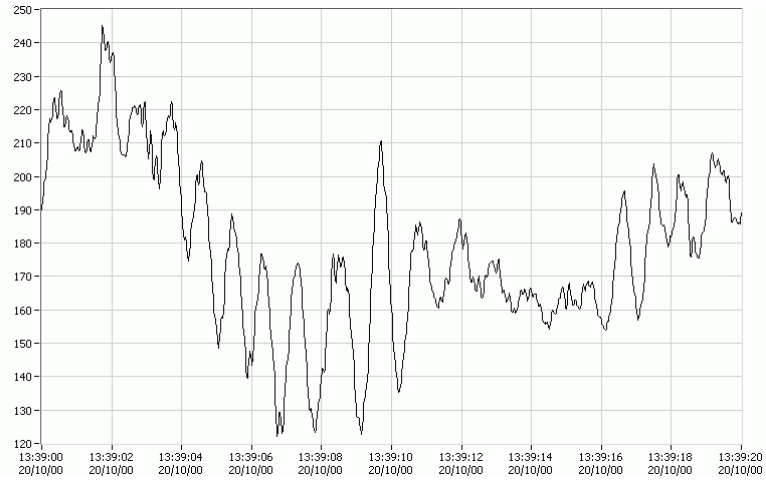

Fig. 1. Active power of a 750 kW wind turbine for wind speeds around 6,7 m/ s during 20 s.

Cyclic variations are usually characterized with their Fourier transforms (Gardner, 1994). Moreover, turbulence is also characterized through its auto spectral density, which is basically the Fourier transform of its autocorrelation. Periodic fluctuations appear as narrow peaks at their harmonic frequencies in the spectrum, whereas random fluctuations (which have neither a periodic pattern nor a characteristic frequency) can be associated with the tendency of the smoothed spectrum. Thus, the magnitude and frequency of the cyclic fluctuations can be characterized for each turbine model and wind regime (Mur-Amada, 2009).
Weather evolution is the outcome of slow and complex atmospheric processes. Since weather evolution has a strong non-linear behaviour, it will not be considered in this chapter.

1.3 Fluctuations induced by the wind turbulence

Many fluctuations in the power output are strongly related to wind fluctuations, especially at low frequencies (slow fluctuations). The wind spectrum is a common way to characterize the frequency content of the turbulence present in the wind as it flows around an anemometer. The wind is usually measured in a fixed point, but the wind varies along a wind farm, not only due to the obstacles and orography, but also due to the turbulent nature of wind.
Taylor's hypothesis of frozen turbulence is a simple model that relates spatial and temporal variations of the wind. This hypothesis can be used to reconstruct the approximate spatial structure of wind from measurements with an anemometer fixed at a point in space.
In fact, wind irregularities experienced by a turbine are also perceived by the next turbines (usually with diverse magnitude and with some time delay). The area of influence of the turbulence is related to the value of wind speed deviations (Cushman-Roisin, 2007). Higher wind fluctuations usually imply larger spatial extent. Therefore, wind fluctuations are usually experienced in close turbines with some time lag/ lead Δt' In Taylor's Hypothesis of "frozen turbulence", the gust travel time in the wind direction Δt' is the distance in longitudinal direction divided by the wind speed (see Fig. 2). The wind measured at the tower of Fig. 2 varies in 10 s due to a perturbation 100 m long travelling at the wind speed.

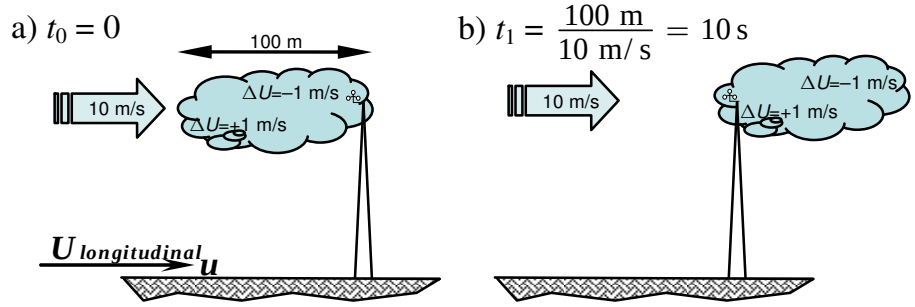

Fig. 2. Example of a idealized eddy of 100 m (represented by a cloud) passing through a meteorological mast according to Taylor's Hypothesis of "frozen turbulence".

If the fluctuation arrives to another turbine inside the time interval [$-\Delta t$, $+\Delta t$], then the phase uncertainty in the frequency domain is [$-2\pi f \Delta t$, $+2\pi f \Delta t$] radians, where f is the considered frequency. When $f > 0{,}5/\ \Delta t$, the phase is undetermined because the uncertainty of the phase excess [$-\pi$, $+\pi$] (i.e. a cycle). At frequencies a few times higher than $0{,}5/\ \Delta t$, the fluctuation of

frequency f is experienced by other turbines with a random phase difference almost uniformly distributed and with comparable amplitude. In other words, the phase of the fluctuations in the frequency domain are uncorrelated stochastically at $f > 0{,}5/\Delta t$ although the amplitude could show a systematic behaviour. The spatial and temporal coherence statistically quantifies the variations of wind in different points in space or in separate moments of time.

For convenience, the wind is sometimes assumed barely uniform in the area swept by the turbine. Based on this approximation, the *equivalent wind* is defined as the one that produces the same effects that the non-uniform real wind field. Although the wind field cannot be directly measured, its effects can be deduced from an equivalent wind that is usually derived from the measurements of an anemometer, because variations in time and space are related by the air flow dynamics.

The equivalent wind speed contains a stochastic component due to the effects of turbulence, a rotational component due to the wind shear and the tower shadow and the average value of the wind in the swept area, considered constant in short intervals. The rotational effects (wind shear and tower effect) are barely related to wind turbulence. Since they interact with the drive-train and control dynamics, they are modelled as an additional term in the oscillations. The rotational/ vibration/ control dynamics are introduced in the equivalent wind as a mathematical artifice to reproduce the power oscillations observed in the turbine output. This simplification works relatively well since the vibration turbine dynamics randomize the real dependence of the generator torque with the rotor angle.

The turbulence does not show characteristic frequencies and the wind spectrum is quite smooth from very low frequencies up to tenths of Hertzs. In contrast, rotational/ vibration/ control oscillations in the power output exhibit a more repetitive pattern with determinate characteristic frequencies. Apart from their frequency distribution, turbulence and other oscillations have similar stochastic properties and they can be modelled with the same mathematical tools.

The combination of the small signal model and the wind coherence permits to derive the spatial averaging of random wind variations. The stochastic behaviour of wind links the overall behaviour of a large number of turbines with the behaviour of a single turbine.

It should be noted that the travel time of the turbulence between the turbines is the very reason why fast fluctuations of turbine power generated by the turbulence are smoothed in the wind farm output. That is also the reason why a Gaussian processes is well suited to model the power fluctuations across a wind farm. Thus, the analysis carried out in this chapter is in the frequency domain for convenience. Moreover, this behaviour also relates the dimensions and geometry of the wind farm with the cut-off frequency of the smoothing (the smoothing depends also on the wind coherence and direction).

The auto spectral density of the equivalent wind of a cluster of turbines can be obtained from the wind spectra, the parameters of an isolated turbine, lateral and longitudinal dimensions of the cluster region and the decay factor of the spatial coherence.

Fluctuations due to the real wind field along the swept area, vibrations and control effects are added to the equivalent wind modifying its spectra. Thus, they can be aggregated in the equivalent wind, provided a turbine transfer function among the power output and the equivalent wind is stated. The turbine transfer function transforms the equivalent wind oscillations into power oscillations. This simplification works relatively well since the turbine vibration dynamics randomize the turbine output and the high frequency turbulence at different turbines has a similar a stochastic behaviour than the

rotational/ vibration/ control oscillations: at high frequencies, fluctuations from turbulence, vibration, generator dynamics and control are fairly independent between turbines, statistically speaking.
The combination of the small signal model and the wind coherence permits to derive the spatial averaging of random wind variations. Since fast turbulence and rotation/ vibration/ control oscillations are almost stochastically independent among the farm turbines, their outcome can be assessed analogously, although their respective sources are very different physical phenomena.
Thus, the overall behaviour of a turbine cluster (with more than 8 turbines) can be derived from the behaviour of a single turbine using a Gaussian model. The wind farm admittance is the ratio of the fluctuations observed in the farm output respect the typical behaviour of one of its turbines. The wind farm admittance can be estimated from experimental measurements or from parameters of an isolated turbine, lateral and longitudinal dimensions of the cluster region and the decay factor of the spatial coherence. Although the model proposed is an oversimplification of the actual behaviour of a group of turbines scattered across an area, this model quantifies the influence of the spatial distribution of the turbines in the smoothing and in the frequency content of the aggregated power. This stochastic model is in agreement with the experimental data presented at the end of this chapter.

1.4 Interaction of wind with turbine dynamics

The interaction between wind fluctuations and the turbine is very complex and a thorough model of the turbine, generator and control system is needed for simulating the influence of wind turbulence in power output (Karaki et al., 2002; Vilar-Moreno, 2003). The control scheme and its optimized parameters are proprietary and difficult to obtain from manufacturers and complex to induce from measurements usually available.
The turbine and micro-meteorological dynamics transform the combination of periodic and random wind variations into stochastic fluctuations in the power. These variations can be divided into equivalent wind variations and almost periodic events such as vibration, blade positions, etc. Turbulence, turbine wakes, gusts... are highly random and do not show a definite frequency (Sørensen et al., 2002; Sørensen et al., 2008). Non-cyclic power variations are usually regarded as the outcome of the random component of the wind. They concern the control (short term prediction) and the forecast (long horizon prediction). Artificial Intelligence techniques and advanced filtering have been used for forecasting. Power fluctuations of frequency around 8 Hz can eventually produce flicker in very weak networks (Thiringer et al., 2004; Amaris & Usaola, 1997).
Both current and power can be measured directly, they can be statistically characterized and they are directly related to power quality. Current is transformed and its level depends on transformer ratio and actual network voltage. In contrast, power flows along transformers and networks without being altered except for some efficiency losses in the elements. That is why linearized power flows in the frequency domain are used in this chapter for characterizing experimentally the electrical behaviour of wind turbines.

1.5 Major difficulties in the fluctuation characterization

A priori estimation of power fluctuations requires thorough models of the wind turbines and turbulence. However, an empirical analysis is much simpler since distinct fluctuation

sources usually present characteristic frequencies or some trend in the spectrum. In the following sections, a phenomenological and pragmatic approach will be applied to draw some conclusions and to extrapolate results from empirical studies to general cases.

The tower shadow, wind shear, rotor asymmetry and unbalance, blade misalignments produce a torque modulation dependent on turbine angle. This torque is filtered by turbine dynamics and the influence in output power can be complex. The signals cannot be considered truly periodic because neither the characteristic frequencies are constant (rotor speed is not constant and hence, the frequency of fluctuations induced by rotational effects) nor the frequencies are harmonically related. Some frequencies cannot be expressed as multiple of the others because the tower, blades and cinematic train present characteristic structural resonance frequencies different from the blade passing the tower frequency, f_{blade}. Moreover, turbine control, electric generator and power electronics introduce oscillations at other frequencies.

The turbulence adds a "coloured noise" overimposed to the former oscillatory modes, modulating cyclic vibrations and influencing rotor speed. The actual power is the outcome of many processes that interact and the analysis in the frequency domain is a simplifying approximation of a system driven by stochastic differential equations.

The first problem when analyzing power variations is that the contributions from rotor sampling, vibration modes and turbulence-driven variations are aggregated.

The second difficulty is the fact that frequencies of almost cyclic contributions are neither fixed nor are they multiple. Fourier coefficients are defined for periodic signals, but the sum of periodic components not harmonically related is no longer periodic.

The third difficulty is that frequencies of contributions are overlapped. Fortunately, characteristic frequencies (resonance and blade frequencies and its harmonics) have narrow margins for given operational conditions, producing peaks in the spectrum where one contribution usually predominates over the rest.

The forth difficulty is the turbulence, that introduces a non-periodic stochastic behaviour interacting with periodic signals. Different mathematical tools are customarily used for periodic and stochastic signals, increasing the difficulty of the analysis of these mixed-type signals.

The cyclic fluctuations of the turbine power can be considered in the *fraction-of-time* probability framework as the sum of sets of signals with different periods with additive stationary coloured noise and, hence, almost cyclostationary (Gardner et al, 2006). Since wind power is formed by the superposition of several almost cyclostationary signals whose periods are not harmonically related, wind power is *polycyclostationary*.

2. Mathematical framework and notation

2.1 Model assumptions

According to (Cidrás et al., 2002), voltage drops can only induce synchronized power fluctuations in a weak electrical network with a very steady and a very uniformly distributed wind. Most grid codes have been modified to minimize the simultaneous loss of generation during special events such as breaker tripping, grid transients, sudden voltages changes, etc. Except during the previous events, the synchronization of power fluctuations from a cluster of turbines is primarily due to wind variations that are slow enough to affect several turbines inside a wind farm.

Experimental measurements have corroborated that blade synchronisation is unusual. In addition, fluctuations due to turbine vibration, dynamics and control can be considered statistically independent between turbines, whereas turbulence and weather dynamics are partially correlated. Fortunately, slow fluctuations can be linked to equivalent wind fluctuations through a quasi-static approximation based on the power curve of the turbines. As an outcome, the total fluctuation from an area is best characterized as a stochastic signal even though the fluctuations from single turbines have strong cyclic components. In other words, the transformation of cyclic components into stochastic components eases the treatment of wind farm power fluctuations.

For convenience, the signal duration will be considered short enough to be stationary (atmospheric dynamics will be supposed not to change considerably during the sample). Therefore, the average power (which corresponds to the zero frequency component of the sample) will be considered a known parameter.

a) Stochastic spectral phasor density of the active power

If $P(t)$ is the active power recorded in $0 \le t \le T$, its conventional Fourier transform, denoted by **F**, is scaled by a factor $1/\sqrt{T}$ to achieve an spectral measure whose main statistical properties do not depend on the sample duration T.

$$\vec{P}(f) \equiv P(f)\, e^{j\varphi(f)} \equiv \frac{1}{\sqrt{T}} \int_0^T P(t) e^{-j2\pi f\, t} dt = \frac{1}{\sqrt{T}} \mathbf{F}\left\{ P(t) \right\} \tag{1}$$

The factor $1/\sqrt{T}$ is between unity –used for pulses and signals of bounded energy– and $1/T$ –used in the Fourier coefficients of pure periodic signals–.

Fortunately, definition (1) has the advantage that the variance of $\vec{P}(f)$ is the two-sided auto spectral density, $\left\langle |\vec{P}(f)|^2 \right\rangle = PSD_P(f)$, which is independent of sample length T and it characterizes the process. $\vec{P}(f)$ will be referred as stochastic spectral phasor density of the active power or just the (stochastic) phasor for short.

Historically, the term "power spectral density" was coined when the signal analyzed $P(t)$ was the electric or magnetic field of a wave or the voltage output of an antenna connected to a resistor *R*. The power transferred to the load R at frequencies between $f - \Delta f/2$ and $f + \Delta f/2$ was $2\Delta f \cdot PSD_P(f)/R$ –that is proportional to $PSD_P(f)$ and the frequency interval. If $P(t)$ is the electric or magnetic field of a wave, then the power density at frequency *f* of that wave is also proportional to $\Delta f \cdot PSD_P(f)$.

In this chapter, $P(t)$ represents the power output of a turbine or a wind farm. The root mean square value (RMS for short) of power fluctuations at frequencies between $f - \Delta f/2$ and $f + \Delta f/2$ is $|\vec{P}(f)| \cdot \sqrt{2 \cdot \Delta f}$. Power variance inside the previous frequency range is $PSD_P(f) \cdot \Delta f$. Hence, $PSD_P(f)$ in this chapter does not represent a power spectral density and this term can lead to misinterpretations. Therefore, $PSD_P(f)$ will be referred in this chapter as the *auto* spectral density although the acronym *PSD* (from Power Spectral Density) is maintained because it is widespread. Sometimes $PSD_P(f)$ will be replaced by $\sigma_P^2(f)$ to emphasize that it represents the *variance* spectral density of signal *P* at frequency *f*.

Fig. 3. shows the estimated *PSD* from 13 minute operation of a squirrel cage induction generator (SCIG) directly coupled to the grid (a portion of the original data is plotted in Fig. 1). The original auto spectrum is plotted in grey whereas the estimated *PSD* is in thin black

(linearly averaged periodogram in squared effective watts of real power per hertz). The trend is plotted in thick red, the accumulated variance is plotted in blue, and the tower shadow frequency is marked in yellow.

The instantaneous output of a wind farm or turbine can be expressed in frequency components using stochastic spectral phasor densities. As aforementioned, experimental measurements indicate that wind power nature is basically stochastic with noticeable fluctuating periodic components.

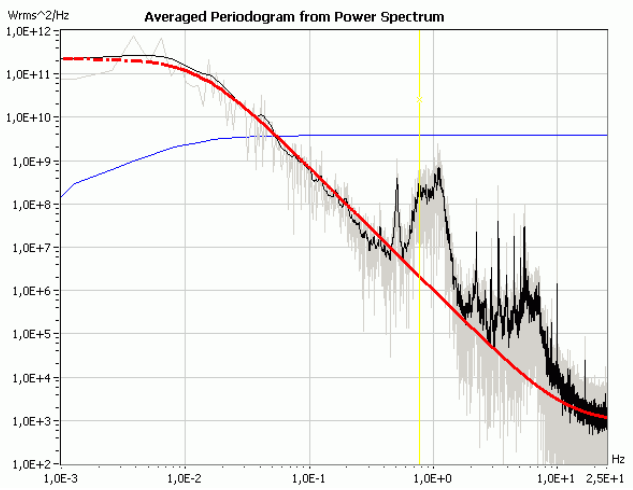

Fig. 3. $PSD_P+(f)$ parameterization of active power of a 750 kW wind turbine for wind speeds around 6,7 m/ s (average power 190 kW) computed from 13 minute data.

The signal in the time domain can be computed from the inverse Fourier transform:

$$P(t)=\sqrt{T}\int_{-\infty}^{\infty}\vec{P}(f)\,e^{j2\pi f\,t}df \underset{\vec{P}(f)=\vec{P}^{*}(-f)}{=} 2\sqrt{T}\int_{0}^{\infty}P(f)\cos\left[2\pi f\,t+\varphi(f)\right]df \qquad (2)$$

An analogue relation can be derived for reactive power and wind, both for continuous and discrete time. Standard FFT algorithms use two sided spectra, with negative frequencies in the last half of the output vector. Thus, calculus will be based on two-sided spectra unless otherwise stated, as in (2). In real signals, the negative frequency components are the complex conjugate of the positive one and a ½ scale factor may be applied to transform one to two-sided magnitudes.

b) Spectral power balance in a wind farm

Fluctuations at the point of common coupling (PCC) of the wind farm can be obtained from power balance equations for the average complex power of the wind farm.

Neglecting the increase in power losses in the grid due to fluctuating generation, the sum of oscillating power from the turbines equals the farm output undulation. Therefore, the complex sum of the frequency components of each turbine $\vec{P}_{turbine\ i}(f)$ totals the approximate farm output, $\vec{P}_{farm}(f)$:

$$\vec{P}_{farm}(f) \cong \sum_{i=1}^{N_{turbines}} \frac{\partial P_{farm}}{\partial P_{turbine\ i}} \vec{P}_{turbine\ i}(f) \approx \sum_{i=1}^{N_{turbines}} \eta_i \vec{P}_{turbine\ i}(f) = \sum_{i=1}^{N_{turbines}} \eta_i P_{turbine\ i}(f) e^{j\varphi_i(f)} \quad (3)$$

For usual wind farm configurations, total active losses at full power are less than 2% and reactive losses are less than 20%, showing a quadratic behaviour with generation level (Mur-Amada & Comech-Moreno, 2006). A small-signal model of power losses due to fluctuations inside the wind farm can be derived (Kundur et al. 1994), but since they are expected to be up to 2% of the fluctuation, the increase of power losses due to oscillations can be neglected in the first instance. A small signal model can be used to take into account network losses multiplying the turbine phasors in (3) by marginal efficiency factors $\eta_i = \partial P_{farm} / \partial P_{turbine\ i}$ estimated from power flows with small variations from the mean values using methodologies as the point-estimate method (Su, 2005; Stefopoulos et al., 2005). Typical values of η_i are about 98% for active power and about 85% for reactive power. In some expressions of this chapter, the efficiency has been set to 100% for clarity in the formulas.

In some applications, we encounter a random signal that is composed of the sum of several random sinusoidal signals, e.g., multipath fading in communication channels, clutter and target cross section in radars, interference in communication systems, wave propagation in random media and channels, laser speckle patterns and light scattering and summation of random current harmonics such as the ones produced by high frequency power converters of wind turbines (Baghzouz et al., 2002; Tentzerakis & Papathanassiou, 2007).

Any random sinusoidal signal can be considered as a random phasor, i.e., a vector with random length and angle. In this way, the sum of random sinusoidal signals is transformed into the sum of 2-D random vectors. So, irrespective of the type of application, we encounter the following general mathematical problem: there are vectors with lengths $P_i = |\vec{P}_i|$ and angles $\varphi_i = Arg(\vec{P}_i)$, in polar coordinates, where P_i and φ_i are random variables, as in (3) and Fig. 4. It is desired to obtain the probability density function (pdf) of the modulus and argument of the resulting vector. A comprehensive literature survey on the sum of random vectors can be obtained from (Abdi, 2000).

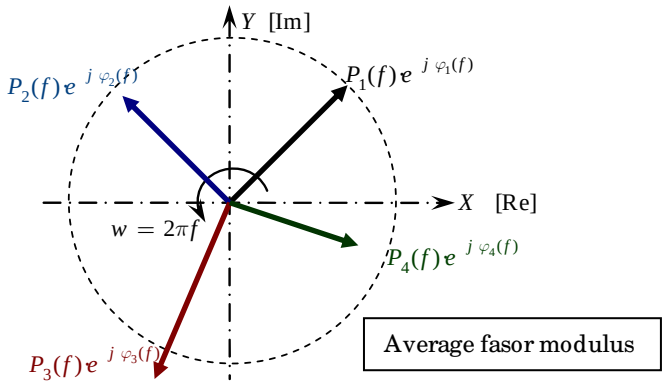

Fig. 4. Model of the phasor diagram of a park with four turbines with a fluctuation level $P_i(f)$ and random argument $\varphi_i(f)$ revolving at frequency f.

The vector sum of the four phasor in Fig. 4 is another random phasor corresponding to the farm phasor, provided the farm network losses are negligible. If some conditions are met, then the farm phasor can be modelled as a complex normal variable. In that case, the phasor amplitude has a Rayleigh distribution. The frequency $f = 0$ corresponds to the special case of the average signal value during the sample.

c) One and two sided spectra notation

One or two sided spectra are consistent –provided all values refer exclusively either to one or to two side spectra. Most differences do appear in integral or summation formulas – if two-sided spectra is used, a factor 2 may appear in some formulas and the integration limits may change from only positive frequencies to positive and negative frequencies.
One-sided quantities are noted in this chapter with a + in the superscript unless the differentiation between one and two sided spectra is not meaningful. For example, the one-sided stochastic spectral phasor density of the active power at frequency f is:

$$\left|\vec{P}^{+}(f)\right| = \left|\vec{P}\ (f)\right| + \left|\vec{P}\ (-f)\right| = 2\left|\vec{P}\ (f)\right| \tag{4}$$

In plain words, the one-sided density is twice the two-sided density. For convenience, most formulas in this chapter are referred to two-sided values.

d) Case study

Fig. 5 to Fig 8 show the power fluctuations of a wind farm composed by 27 wind turbines of 600 kW with variable resistance induction generator from VESTAS (Mur-Amada, 2009). The data-logger recorded signals either at a single turbine or at the substation. In either case, wind speed from the meteorological mast of the wind farm was also recorded.
The record analyzed in this subsection corresponds to date 26/ 2/ 1999 and time 13:52:53 to 14:07:30 (about 14:37 minutes). The average blade frequency in the turbines was $f_{blade} \approx$ 1,48 ±0,03 Hz during the interval. The wind speed, measured in a meteorological mast at 40 m above the surface with a propeller anemometer, was U_{wind} = 7,6 m/ s ±2,0 m/ s (expanded uncertainty).
The oscillations due to rotor position in Fig. 5 are not evident since the total power is the sum of the power from 26 unsynchronized wind turbines minus losses in the farm network. Fig. 6 shows a rich dynamic behaviour of the active power output, where the modulation and high frequency oscillations are superimposed to the fundamental oscillation.

3. Asymptotic properties of the wind farm spectrum

The fluctuations of a group of turbines can be divided into the correlated and the uncorrelated components.
On the one hand, slow fluctuations ($f < 10^{-3}$ Hz) are mainly due to meteorological dynamics and they are widely correlated, both spatially and temporally. Slow fluctuations in power output of nearby farms are quite correlated and wind forecast models try to predict them to optimize power dispatch.
On the other hand, fast wind speed fluctuations are mainly due to turbulence and microsite dynamics (Kaimal, 1978). They are local in time and space and they can affect turbine control and cause flicker (Martins et al., 2006). Tower shadow is usually the most noticeable fluctuation of a turbine output power. It has a definite frequency and, if the blades of all turbines of an area became eventually synchronized, it could be a power quality issue.

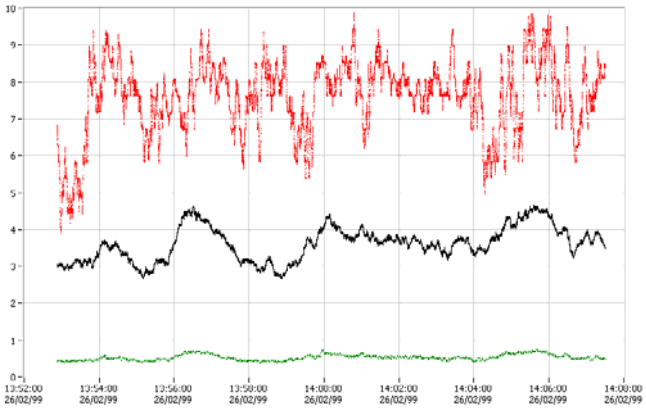

Fig. 5. Time series (from top to bottom) of the active power P [MW] (in black), wind speed U_{wind} [m/ s] at 40 m in the met mast (in red) and reactive power Q [MVAr] (in dashed green).

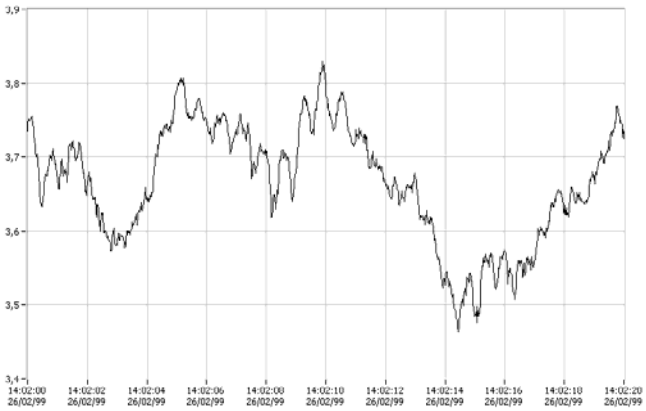

Fig. 6. Detail of the wind farm active power during 20 s at the wind farm.

The phase $\varphi_i(f)$ implies the use of a time reference. Since fluctuations are random events, there is not an unequivocal time reference to be used as angle reference. Since fluctuations can happen at any time with the same probability –there is no preferred angle $\varphi_i(f)$–, the phasor angles are random variables uniformly distributed in $[-\pi,+\pi]$ (i.e., the system exhibits circular symmetry and the stochastic process is cyclostationary). Therefore, the relevant information contained in $\varphi_i(f)$ is the relative angle difference among the turbines of the farm (Li et al., 2007) in the range $[-\pi,+\pi]$, which is linked to the time lag among fluctuations at the turbines.

The central limit for the sum of phasors is a fair approximation with 8 or more turbines and Gaussian process properties are applicable. Therefore, the wind farm spectrum converges asymptotically to a complex normal distribution, denoted by $\mathbb{C}N\left(0, \sigma_{Pfarm}(f)\right)$. In other words, $\mathrm{Re}[\vec{P}^{+}_{farm}(f)]$ and $\mathrm{Im}[\vec{P}^{+}_{farm}(f)]$ are independent random variables with normal distribution.

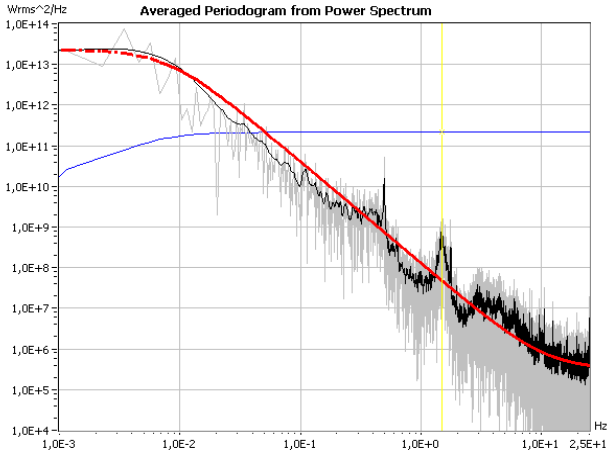

Fig. 7. $PSD_P+(f)$ parameterization of real power of a wind farm for wind speeds around 7,6 m/ s (average power 3,6 MW) computed from data of Fig. 5.

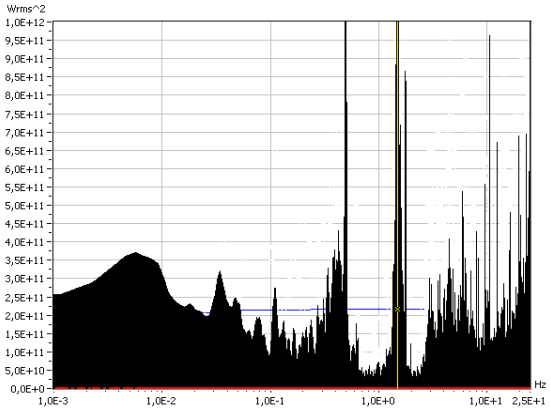

Fig. 8. Contribution of each frequency to the variance of power computed from Fig. 5 (the area bellow $f \cdot PSD_P+(f)$ in semi-logarithmic axis is the variance of power).

$$\vec{P}^{+}_{farm}(f) \sim \mathbb{C}N\left(0, \sigma_{farm}(f)\right) \tag{5}$$

Thus, the one-sided amplitude density of fluctuations at frequency f from N turbines, $\left|\vec{P}^{+}_{farm}(f)\right|$, is a Rayleigh distribution of scale parameter $\sigma_{Pfarm}(f) = \langle|\vec{P}^{+}_{farm}(f)|\rangle\sqrt{2/\pi}$, where angle brackets $\langle\bullet\rangle$ denotes averaging. In other words, the mean of $\left|\vec{P}^{+}_{farm}(f)\right|$ is $\langle|\vec{P}^{+}_{farm}(f)|\rangle = \sqrt{\pi/2}\ \sigma_{Pfarm}(f)$ where $\sigma_{Pfarm}(f)$ is the RMS value of the phasor projection. The RMS value of the phasor projection $\sigma_{Pfarm}(f)$ is also related to the one and two sided PSD of the active power:

$$\sigma_{Pfarm}(f) = \sqrt{2PSD_{Pfarm}(f)} = \sqrt{PSD^{+}_{Pfarm}(f)} \tag{6}$$

Put into words, the phasor density of the oscillation, $\left|\vec{P}^{+}_{Pfarm}(f)\right|$, has a Rayleigh distribution of scale parameter $\sigma_{Pfarm}(f)$ equal to the square root of the auto spectral density (the equivalent is also hold for two-sided values). The mean phasor density modulus is:

$$\langle|\vec{P}^{+}_{Pfarm}(f)|\rangle \underset{Rayleigh(\sigma_{Pfarm}(f))}{=} \sqrt{\frac{\pi}{2}}\sigma_{Pfarm}(f) \tag{7}$$

For convenience, effective values are usually used instead of amplitude. The effective value of a sinusoid (or its root mean square value, RMS for short) is the amplitude divided by √2. Thus, the average quadratic value of the fluctuation of a wind farm at frequency f is:

$$\left\langle\left|\vec{P}^{+}_{Pfarm}(f)/\sqrt{2}\right|^2\right\rangle = \left\langle\left|\vec{P}^{+}_{Pfarm}(f)\right|^2\right\rangle/2 \underset{Rayleigh[\sigma_N(f)]}{=} \sigma^2_{Pfarm}(f) = PSD^{+}_{Pfarm}(f) \tag{8}$$

If the active power of the turbine cluster is filtered with an ideal *narrowband filter* tuned at frequency f and bandwidth Δf, then *the average effective value* of the filtered signal is $\sigma_{Pfarm}(f)\sqrt{\Delta f}$ and the *average amplitude* of the oscillations is $\langle|\vec{P}^{+}_{farm}(f)|\rangle\cdot\sqrt{\Delta f} = \sigma_{Pfarm}(f)\sqrt{\Delta f\cdot\pi/2}$. The instantaneous value of the filtered signal $P_{Pfarm,f,\Delta f}(t)$ is the projection of the phasor $\vec{P}^{+}_{farm}(f)\,e^{j2\pi f\,t}\sqrt{\Delta f}$ in the real axis. The instantaneous value of the square of the filtered signal, $P^2_{farm,f,\Delta f}(t)$, is an exponential random variable of parameter $\lambda=[\sigma^2_{farm}(f)\Delta f]^{-1}$ and its mean value is:

$$\left\langle P^2_{farm,f,\Delta f}(t)\right\rangle \underset{Exp\ distribution}{=} \lambda = \sigma^2_{Pfarm}(f)\Delta f \tag{9}$$

For a continuous *PSD*, the expected variance of the instantaneous power output during a time interval T is the integral of $\sigma_{Pfarm}(f)$ between $\Delta f = 1/T$ and the grid frequency, according to Parseval's theorem (notice that the factor 1/2 must be changed into 2 if two-sided phasors densities are used):

$$\left\langle P^2_{farm}(t)\right\rangle = \frac{1}{2}\left\langle\int_{1/T}^{f_{grid}}|\vec{P}^{+2}_{farm}(f)|df\right\rangle = \frac{1}{2}\int_{1/T}^{f_{grid}}\langle|\vec{P}^{+2}_{farm}(f)|\rangle df = \int_{1/T}^{f_{grid}}\sigma^2_{farm}(f)df \tag{10}$$

In fact, data is sampled and the expected variance of the wind farm power of duration T can be computed through the discrete version of (10), where the frequency step is $\Delta f = 1/T$ and the time step is $\Delta t = T/m$:

$$\left\langle P^2_{farm}(t)\right\rangle = \frac{1}{2}\left\langle\sum_{k=1}^{m-1}|\vec{P}^{+2}_{farm}(k\Delta f)|\,\Delta f\right\rangle = \frac{1}{2}\sum_{k=1}^{m-1}\langle|\vec{P}^{+2}_{farm}(k\Delta f)|\rangle\Delta f = \sum_{k=1}^{m-1}\sigma^2_{Pfarm}(k\Delta f)\Delta f \tag{11}$$

If a fast Fourier transform is used as a narrowband filter, an estimate of $\sigma^2_{Pfarm}(f)$ for $f = k\,\Delta f$ is $2\Delta f \cdot \langle |FFT_k\{P_{farm}(i\Delta t)\}|^2 \rangle$. In fact, the factor $2\Delta f$ may vary according to the normalisation factor included in the FFT, which depends on the software used. Usually, some type of smoothing or averaging is applied to obtain a consistent estimate, as in Bartlett or Welch methods (Press et al., 2007).

The distribution of $\left\langle P^2_{farm}(t) \right\rangle$ can be derived in the time or in the frequency domain. If the process is normal, then the modulus and phase of $\vec{P}^{+}_{farm}(f_k)$ are not linearly correlated at different frequencies f_k. Then $\left\langle P^2_{farm}(t) \right\rangle$ is the sum in (11) or the integration in (10) of independent Exponential random variables that converges to a normal distribution with mean $\left\langle P^2_{farm}(t) \right\rangle$ and standard deviation $\sqrt{2}\left\langle P^2_{farm}(t) \right\rangle$.

In farms with a few turbines, the signal can show a noticeable periodic fluctuation shape and the auto spectral density $\sigma^2_{Pfarm}(f)$ can be correlated at some frequencies. These features can be discovered through the bispectrum analysis. In such cases, $\left\langle P^2_{farm}(t) \right\rangle$ can be computed with the algorithm proposed in (Alouini et al., 2001).

4. Sum of partially correlated phasor densities of power from several turbines

4.1 Sum of fully correlated and fully uncorrelated spectral components

If turbine fluctuations at frequency f of a wind farm with N turbines are completely synchronized, all the phases have the same value $\varphi(f)$ and the modulus of fully correlated fluctuations $|\vec{P}^{+}_{i,\,corr}(f)|$ sum arithmetically:

$$|\vec{P}^{+}_{farm,\,corr}(f)| = \left| \sum_{i=1}^{N} \eta_i \vec{P}^{+}_{i,\,corr}(f) \right| = \sum_{i=1}^{N} |\eta_i \vec{P}^{+}_{i,\,corr}(f)| \tag{12}$$

If there is no synchronization at all, the fluctuation angles $\varphi_i(f)$ at the turbines are stochastically independent. Since $\vec{P}_{i,\,uncorr}(f)$ has a random argument, its sum across the wind farm will partially cancel and inequality (13) holds true.

$$|\vec{P}^{+}_{farm,\,uncorr}(f)| = \left| \sum_{i=1}^{N} \eta_i \vec{P}^{+}_{i,\,uncorr}(f) \right| < \sum_{i=1}^{N} \eta_i |\vec{P}^{+}_{i,\,uncorr}(f)| \tag{13}$$

This approach remarks that correlated fluctuations adds arithmetically and they can be an issue for the network operation whereas uncorrelated fluctuations diminish in relative terms when considering many turbines (even if they are very noticeable at turbine terminals).

A) Sum of uncorrelated fluctuations

The fluctuation of power output of the farm is the sum of contributions from many turbines (3), which are mainly uncorrelated at frequencies higher than a tenth of Hertz.

The sum of N independent phasors of random angle of N equal turbines in the farm converges asymptotically to a complex Gaussian distribution, $\vec{P}_{farm}(f) \sim \mathbb{C}N[0, \sigma_{Pfarm}(f)]$, of null mean and standard deviation $\sigma_{farm}(f) = \sqrt{\eta N}\,\sigma_1(f)$, where $\sigma_1(f)$ is the mean RMS fluctuation at a single turbine at frequency f and η is the average efficiency of the farm network. To be precise, the variance $\sigma_1{}^2(f)$ is half the mean squared fluctuation amplitude

at frequency f, $\sigma_1^2(f) = \frac{1}{2}\left\langle \left|\vec{P}_{turbine\ i}(f)\right|^2 \right\rangle = \left\langle \mathrm{Re}^2\left[\vec{P}_{turbine\ i}(f)\right]\right\rangle = \left\langle \mathrm{Im}^2\left[\vec{P}_{turbine\ i}(f)\right]\right\rangle$. Therefore, the real and imaginary phasor components $\mathrm{Re}[\vec{P}_{farm}(f)]$ and $\mathrm{Im}[\vec{P}_{farm}(f)]$ are independent real Gaussian random variables of standard deviation $\sigma_{Pfarm}(f)$ and null mean since phasor argument is uniformly distributed in $[-\pi,+\pi]$. Moreover, the phasor modulus $\left|\vec{P}_{farm}(f)\right|$ has $Rayleigh[\sigma_{Pfarm}(f)]$ distribution. The double-sided power spectrum $\left|\vec{P}_{farm}(f)\right|^2$ is an $Exponential\left[\lambda = \frac{1}{2}\sigma_{Pfarm}^{-2}(f)\right]$ random vector of mean $\left\langle \left|\vec{P}_{farm}(f)\right|^2 \right\rangle = 2\sigma_{Pfarm}^2(f) = \frac{1}{2}PSD_{Pfarm}(f)$ (Cavers, 2003).

The estimate from the periodogram is the moving average of $N_{aver.}$ exponential random variables corresponding to adjacent frequencies in the power spectrum vector. The estimate is a Gamma random variable. If the PSD is sensibly constant on $N_{aver}\Delta f$ bandwidth, then the PSD estimate has the same mean as the original PSD and the standard deviation is $\sqrt{N_{aver.}}$ times smaller (i.e., the estimate has lower uncertainty at the cost of lower frequency resolution).

4.2 Sum of partially linearly correlated spectral components

Inside a farm, the turbines usually exhibit a similar behaviour for a given frequency f and the PSD of each turbine is expected to be fairly similar. However, the phase differences among turbines do vary with frequency. Slow meteorological variations affect all the turbines with negligible time lag, compared to characteristic time frame of weather systems (i.e., the phasors $\vec{P}_{turbine}(f)$ have the same phase). Turbulences with scales significantly smaller than the turbine distances have uncorrelated phases. Fluctuations due to rotor positions also show uncorrelated phases provided turbines are not synchronized.

$$\left\langle P_{turbine}^{+}(f)\right\rangle^2 = \left\langle P_{turb,corr}^{+}(f)\right\rangle^2 + \left\langle P_{turb,uncorr}^{+}(f)\right\rangle^2 \tag{14}$$

If the number of turbines N >4 and the correlation among turbines are linear, the central limit is a good approximation. The correlated and uncorrelated components sum quadratically and the following relation is applicable:

$$\left\langle \left|\vec{P}_{farm}^{+}(f)\right|^2 \right\rangle \approx \left(\eta N\right)^2 \left\langle \left|\vec{P}_{turb,\,corr}^{+}(f)\right|^2 \right\rangle + \eta N \left\langle \left|\vec{P}_{turb,\,uncorr}^{+}(f)\right|^2 \right\rangle \tag{15}$$

where N is the number of turbines in the farm (or in a group of close farms) and η is the average efficiency of the farm network (typical values are about 98% for active power and about 85% for reactive power). Since phasor densities sum quadratically, (14) and (15) are concisely expressed in terms of the PSD of correlated and uncorrelated components of phasor density:

$$PSD_{farm}(f) \approx \left(\eta N\right)^2 PSD_{turb,\,corr}(f) + \eta N \cdot PSD_{turb,\,uncorr}(f) \tag{16}$$

$$PSD_{turb}(f) = PSD_{turb,\,corr}(f) + PSD_{turb,\,uncorr}(f) \tag{17}$$

The correlated components of the fluctuations are the main source of fluctuation in large clusters of turbines. The farm admittance $J(f)$ is the ratio of the mean fluctuation density of the farm, $\left\langle \left| \vec{P}_{farm}(f) \right| \right\rangle$, to the mean turbine fluctuation density, $\left\langle |P^{+}_{turbine}(f)| \right\rangle$.

$$J(f) = \frac{\left\langle |P^{+}_{farm}(f)| \right\rangle}{\left\langle |P^{+}_{turbine}(f)| \right\rangle} \approx \sqrt{\frac{PSD_{Pfarm}(f)}{PSD_{Pturbine}(f)}} \tag{18}$$

Note that the phase of the admittance $J(f)$ has been omitted since the phase lag between the oscillations at the cluster and at a turbine depend on its position inside the cluster. The admittance is analogous to the expected gain of the wind farm fluctuation respect the turbine expected fluctuation at frequency f (the ratio is referred to the mean values because both signals are stochastic processes).
Since turbine clusters are not negatively correlated, the following inequality is valid:

$$\sqrt{\eta N} \lesssim J(f) \lesssim \eta N \tag{19}$$

The squared modulus of the admittance $J(f)$ is conveniently estimated from the PSD of the turbine cluster and a representative turbine using the cross-correlation method and discarding phase information (Schwab et al., 2006):

$$J^2(f) = \frac{PSD_{Pfarm}(f)}{PSD_{Pturb}(f)} = \left(\eta N\right)^2 \frac{PSD_{turb,corr}(f)}{PSD_{turb}(f)} + \eta N \frac{PSD_{turb,uncorr}(f)}{PSD_{turb}(f)} \tag{20}$$

If the PSD of a representative turbine, $PSD_{Pturb}(f)$, and the PSD of the farm $PSD_{Pfarm}(f)$ are available, the components $PSD_{turb,corr}(f)$ and $PSD_{turb,uncorr}(f)$ can be estimated from (16) and (17) provided the behaviour of the turbines is similar.
At $f \ll$ 0,01 Hz, fluctuations are mainly correlated due to slow weather dynamics, $PSD_{turb,uncorr}(f) \ll PSD_{turb,corr}(f)$, and the slow fluctuations scale proportionally $PSD_{Pfarm}(f) \approx (\eta N)^2 PSD_{turb,corr}(f)$. At $f >$ 0,01 Hz, individual fluctuations are statistically independent, $PSD_{turb,uncorr}(f) \gg PSD_{turb,corr}(f)$, and fast fluctuations are partially attenuated, $PSD_{Pfarm}(f) \approx \eta N \cdot PSD_{turb,uncorr}(f)$.
An analogous procedure can be replicated to sum fluctuations of wind farms of a geographical area, obtaining the correlated $PSD_{farm,corr}(f)$ and uncorrelated $PSD_{farm,uncorr}(f)$ components. The main difference in the regional model –apart from the scattered spatial region and the different turbine models– is that wind farms must be normalized and an average farm model must be estimated for reference. Therefore, the average farm behaviour is a weighted average of individual farms with lower characteristic frequencies (Norgaard & Holttinen, 2004). Recall that if hourly or even slower fluctuations are studied, meteorological dynamics are dominant and other approaches are more suitable.

4.3 Estimation of wind farm power admittance from turbine coherence

The admittance can be deducted from the farm power balance (3) if the coherence among the turbine outputs is known. The system can be approximated by its second-order statistics

as a multivariate Gaussian process with spectral covariance matrix $\Xi_P(f)$. The elements of $\Xi_P(f)$ are the complex squared coherence at frequency f and at turbines i and j, noted as $\vec{\gamma}_{ij}(f)$. The efficiency of the power flow from the turbine i to the farm output can be expressed with the column vector $\eta_P = [\eta_1, \eta_2, ..., \eta_N]^T$, where ^{T} denotes transpose.
Therefore, the wind farm power admittance $J(f)$ is the sum of all the coherences, multiplied by the efficiency of the power flow:

$$J^2(f) \approx \left| \sum_{i=1}^{N} \sum_{j=1}^{N} \eta_i \eta_j \vec{\gamma}_{ij}(f) \right| = \left| \eta_P^T \ \Xi_P(f) \ \eta_P \right| \tag{21}$$

The squared admittance for a wind farm with a grid layout of n_{long} columns separated d_{long} distance in the wind direction and n_{lat} rows separated d_{lat} distance perpendicular to the wind U_{wind} is:

$$J^2(f) \approx \eta^2 \sum_{i_1=1}^{n_{lat}} \sum_{i_2=1}^{n_{lat}} \sum_{j_1=1}^{n_{long}} \sum_{j_2=1}^{n_{long}} Cos\left[\frac{2\pi(j_2 - j_1) d_{long} f}{U_{wind}} \right] Exp\left[\frac{-f\sqrt{A_{lat}^2 (i_2 - i_1)^2 d_{lat}^2 + A_{long}^2 (j_2 - j_1)^2 d_{long}^2}}{U_{wind}} \right] \tag{22}$$

The admittance computed for Horns Rev offshore wind farm (with a layout similar to Fig. 10) is plotted in Fig. 9. According to (Sørensen et al., 2008), it has 80 wind turbines disposed in a grid of n_{lat} = 8 rows and n_{long} = 10 columns separated by seven diameters in each direction (d_{lat} = d_{long} = 560 m), high efficiency ($\eta \approx$ 100%), lateral coherence decay factor $A_{lat} \approx U_{wind}$/ (2 m/ s), longitudinal coherence decay factor $A_{long} \approx 4$, wind direction aligned with the rows and $U_{wind} \approx$ 10 m/ s wind speed.

4.4 Estimation of wind farm power admittance from the wind coherence

The wind farm admittance $J(f)$ can be approximated from the equivalent farm wind because the coherence of power and wind are similar (the transition frequency between correlated and uncorrelated behaviour is about 10^{-2} Hz for small wind farms). According to (Mur-Amada, 2009), the equivalent wind can be roughly approximated by a multivariate

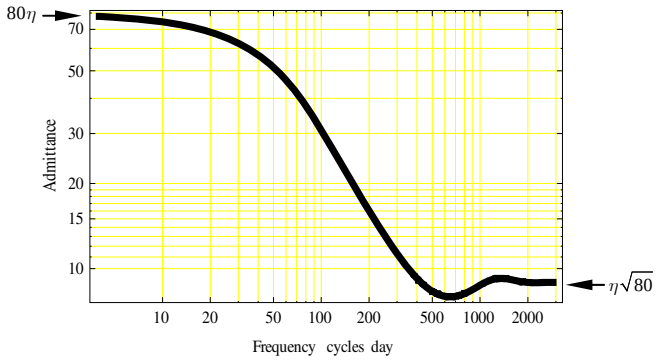

Fig. 9. Admittance for Horns Rev offshore wind farm for 10 m/ s and wind direction aligned with the turbine rows.

Gaussian process with spectral covariance matrix $\Xi_{Ueq}(f)$. Its elements are the complex coherence of effective turbulence at frequency f and at turbines i and j, denoted by $\vec{\gamma}_{ij}(f)$. In this case, the column vector $\eta_{Ueq} = [\eta_1, \eta_2, ..., \eta_N]^T$ should be interpreted as the relative sensitivity of the farm power respect the equivalent wind in each turbine. Therefore, the wind farm power admittance $J(f)$ is the sum of the complex coherence of effective quadratic turbulence among turbines:

$$J^2(f) \approx \left| \sum_{i=1}^{N} \sum_{j=1}^{N} \eta_i \eta_j \vec{\gamma}_{ij}(f) \right| = \left| \eta_{Ueq}^T \; \Xi_{Ueq}(f) \; \eta_{Ueq} \right| \tag{23}$$

For the rectangular region shown in Fig. 10, the admittance is:

$$J^2(f) \approx \eta N \left\{ 1 + (\eta N - 1) H^2(f) \right\} \tag{24}$$

where

$$H^2(f) = \frac{PSD_{Ueq,area}(f)}{PSD_{Ueq,turbine}(f)} = g\left(\frac{A_{lat} b \; f}{\langle U_{wind} \rangle} \right) \mathrm{Re}\left[g\left(\frac{(A_{long} + j2\pi) \; a \; f}{\langle U_{wind} \rangle} \right) \right] \tag{25}$$

$$g(x) = 2\left(-1 + e^{-x} + x \right) / \; x^2 \tag{26}$$

$\langle U_{wind} \rangle$ is the mean wind during the sample, η is the average sensitivity of the power respect the wind and a and b are the dimensions of the wind farm according to Fig. 10. The decay constants for lateral and longitudinal directions are, A_{long} and A_{lat}, respectively. For the Rutherford Appleton Laboratory, (Schlez & Infield, 1998) recommended $A_{long} \approx (15 \pm 5) \; \sigma_{Uwind} / \; \langle U_{wind} \rangle$ and $A_{lat} \approx (17{,}5 \pm 5)$ (m/ s)$^{-1} \sigma_{Uwind}$, where σ_{Uwind} is the standard deviation of the wind speed in m/ s. IEC 61400-1 recommends $A \approx 12$; Frandsen (Frandsen et al., 2007) recommends $A \approx 5$ and Saranyasoontorn (Saranyasoontorn et al., 2004) recommends $A \approx 9{,}7$.

$H^2(f)$ is the quadratic coherence between the equivalent wind of the farm, relative to the turbine. $H(f)$ measures the correlation of the phase difference between the equivalent wind of the farm relative to the turbine at frequency f. If $H(f)$ is unity, the turbine phasors have

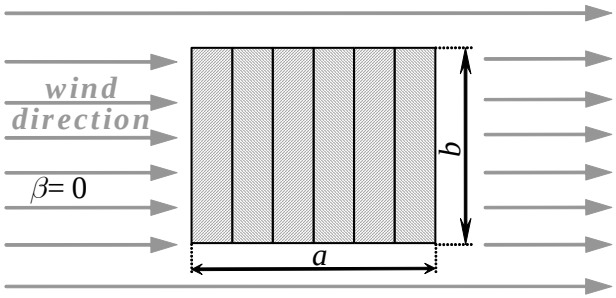

Fig. 10. Wind farm dimensions for the case of frontal wind direction.

the same angle and the turbine fluctuations are synchronized at that frequency. If $H(f)$ is zero, the phasors have uncorrelated arguments and hence, the turbine fluctuations are stochastically uncorrelated at that frequency. Hence, $H(f)$ is the correlation level at frequency f of the fluctuations among the turbines, measured from 0 to 1.
The transition frequency from correlated to uncorrelated fluctuations is obtained solving $H^2(f) = 1/4$. Thus, the cut-off frequency of narrow wind farms with $a \ll b$ is:

$$f_{cut,lat} = 6.83 \frac{\langle U_{wind} \rangle}{bA_{lat}} \tag{27}$$

In the Rutherford Appleton Laboratory (RAL), $A_{lat} \approx (17{,}5 \pm 5)(\text{m/s})^{-1} \sigma_{Uwind}$ and hence $f_{cut,lat} \approx (0{,}42 \pm 0{,}12) \langle U_{wind} \rangle / (\sigma_{Uwind} b)$. A typical value of the turbulence intensity $\sigma_{Uwind} / \langle U_{wind} \rangle$ is around 0,12 and for such value $f_{cut,lat} \sim (3.5 \pm 1)/b$, where b is the lateral dimension of the area in meters. For a narrow farm of b = 3 km, the cut-off frequency is in the order of 1,16 mHz.
In Horns Rev wind farm, $A_{lat} = \langle U_{wind} \rangle / (2 \text{ m/s})$ and hence $f_{cut,lat} \approx 13{,}66/b$, where b is a constant expressed in meters. For a wind farm of b = 3 km, the cut-off frequency is in the order of 4,5 mHz (about four times the estimation from RAL).
In RAL, $A_{long} \approx (15 \pm 5)\ \sigma_{Uwind} / \langle U_{wind} \rangle$. A typical value of the turbulence intensity $\sigma_{Uwind} / \langle U_{wind} \rangle$ is around 0,12 and for such value $A_{long} \approx (1{,}8 \pm 0{,}6)$.

$$f_{cut,long} \underset{A_{long} \sim 1,8}{=} 1,1839 \frac{\langle U_{wind} \rangle}{a A_{long}} \underset{A_{long} = 1.8}{=} 0.6577 \frac{\langle U_{wind} \rangle}{a} \tag{28}$$

For a significative wind speed of $\langle U_{wind} \rangle \sim 10$ m/s and a wind farm of a = 3 km longitudinal dimension, the cut-off frequency is in the order of 2,19 mHz.
In the Høvsøre wind farm, A_{long} = 4 (about twice the value from RAL). The cut-off frequency of a longitudinal area with A_{long} around 4 (dashed gray line in Fig. 11) is:

$$f_{cut,long} \underset{A_{long} \sim 4}{=} 2.7217 \frac{\langle U_{wind} \rangle}{a A_{long}} \underset{A_{long} = 4}{=} 0.6804 \frac{\langle U_{wind} \rangle}{a} \tag{29}$$

For a significative wind speed of $\langle U_{wind} \rangle \sim$ 10 m/s and a wind farm of a = 3 km longitudinal dimension, the cut-off frequency is in the order of 2,26 mHz.
In accordance with experimental measurements, turbulence fluctuations quicker than a few minutes are notably smoothed in the wind farm output. This relation is proportional to the dimensions of the area where the wind turbines are sited. That is, if the dimensions of the zone are doubled, the area is four times the original region and the cut-off frequencies are halved. In other words, *the smoothing of the aggregated wind is proportional to the longitudinal and lateral lengths* (and thus, related to the square root of the area if zone shape is maintained).
In sum, the lateral cut-off frequency is inversely proportional to the site parameters A_{lat} and the longitudinal cut-off frequency is only slightly dependent on A_{long}. Note that the longitudinal cut-off frequency show closer agreement for Høvsøre and RAL since it is dominated by frozen turbulence hypothesis.

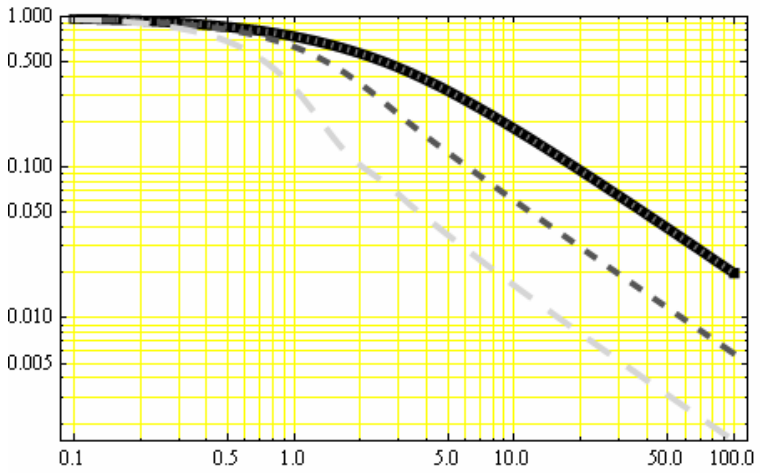

Fig. 11. Normalized ratio $H^2(f)$ for transversal $a \ll b$ (solid thick black line) and longitudinal $a \gg b$ areas (dashed dark gray line for $A_{long} = 4$, long dashed light gray line for $A_{long} = 1{,}8$). Horizontal axis is expressed in either longitudinal or lateral adimensional frequency $a\, A_{long}\, f \,/\, \langle U_{wind} \rangle$ or $b\, A_{lat}\, f \,/\, \langle U_{wind} \rangle$.

However, if transversal or longitudinal smoothing dominates, then the cut-off frequency is approximately the minimum of $f_{cut,lat}$ and $f_{cut,long}$. The system behaves as a first order system at frequencies above both cut-off frequencies, and similar to a ½ order system between $f_{cut,lat}$ and $f_{cut,long}$.

5. Case study: comparison of PSD of a wind farm with respect to one of its turbines during 12 minutes

A literature review on experimental data of power output PSD from wind turbines or wind farms can be found in (Mur-Amada & Bayod-Rujula, 2007), with a parameterization and analysis of the data from very different locations. (Apt, 2007) shows an interesting comparison of the spectrum of the wind power from a wide area.

In this sub-section, the analysis of a case based on (Mur-Amada, 2009) is presented. The similarity of the *PSD* at one turbine and at the overall output of a wind farm of 18 turbines is shown. If the fluctuations at every turbine are independent (i.e. the turbines behaves independently from each other), then the *PSD* of the wind farm is approximately the *PSD* of each turbine multiplied by the number of turbines and by the power flow efficiency.

Each turbine experiments different turbulence levels and wind averages, so a representative turbine should be selected. The time lag between the variations measured in the farm and in the turbine depends on the farm layout. The phase information has been discarded because the phase of ergodic stochastic processes do not contain statistical information.

Fig. 12 shows the power output of the wind farm and the scalled output of one turbine. Since the measured turbine is more exposed to the wind than others turbines, the ratio of the average power of the turbine to the farm is 14 (less than 18, the number of turbines in the farm). There is a clear reduction of the relative variability in the farm output and some slow

oscillations between the turbine and the farm seem to be delayed. In fact, this section will show that the ratio of the fluctuations is about √18 because the measured fluctuations are mainly uncorrelated, the duration of the sample is relatively short (less than 12 minutes) and the wind does not show a noticeable trend during the sample.

If the turbines behave independently from each other and they are similar, then the *PSD* of the wind farm is the *PSD* of one turbine times the number of turbines in the farm and times a power efficiency factor. To test this hypothesis, the farm *PSD* is shown in solid black and the turbine *PSD* times 18 is in dashed green in Fig. 13, with good agreement.

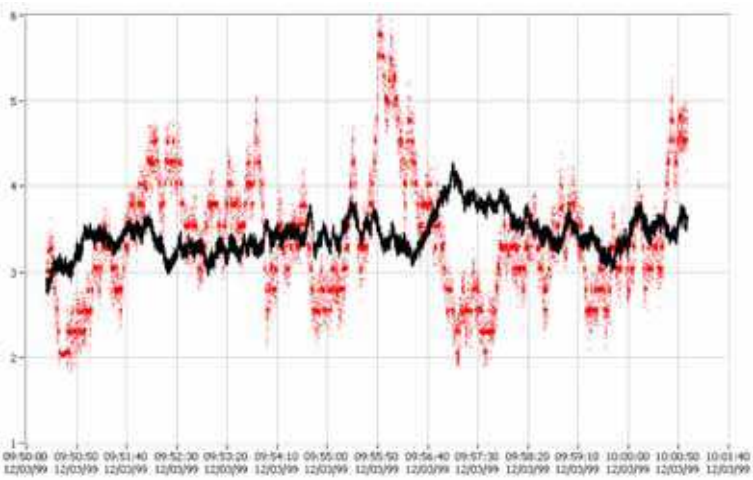

Fig. 12. Power output of the wind farm (in solid black) and the power of the turbine times 14.

Fig. 13 shows that the farm $PSD_{P^+}(f)$ and the scaled turbine $PSD_{P^+}(f)$ agree notably, showing that fluctuations up to 10^{-2} Hz are almost uncorrelated (frequency bellow 10^{-2} Hz is shown in the figure, but its value is biased by the window applied in the *FFT* and the relative short duration of the sample). However, the wind farm *PSD* is a bit lower than 18 times the turbine *PSD*, specially at the peaks and at $f > 2f_{blade}$ (f_{blade} is the frequency of a blade crossing the turbine tower, about 1,54 Hz in this sample). On the one hand, this turbine experiences more cyclic oscillations, partly due to a misalignment of the rotor bigger than the farm average. On the other hand, this turbine produced an average of 1/ 14th of the wind farm power on the series #1 (see Fig. 12). This explain that *PSD* at $f > 2f_{blade}$ is primarily proportional to power output ratio (the farm *PSD* is 14 times the turbine *PSD*).

The real power admittance is shown in Fig. 14. The admittance is the ratio of the farm spectrum to the turbine spectrum of real power and it can be estimated as the square root of the *PSD* ratios. The level √18 has been added in dash-dotted red line to compare with the theoretical value of uncorrelated fluctuations.

In general terms, the assumption of uncorrelated fluctuations at frequencies higher than 10^{-2} Hz is valid: the admittance is approximately √18, the square root of the number of turbines in the farm. At $f > 2f_{blade}$, the admittance is more similar to √14 (the square root of the farm power divided by the turbine power). At $f < 0{,}02$ Hz, the admittance starts drifting from √18, indicating that oscillations at very low frequency are somewhat correlated.

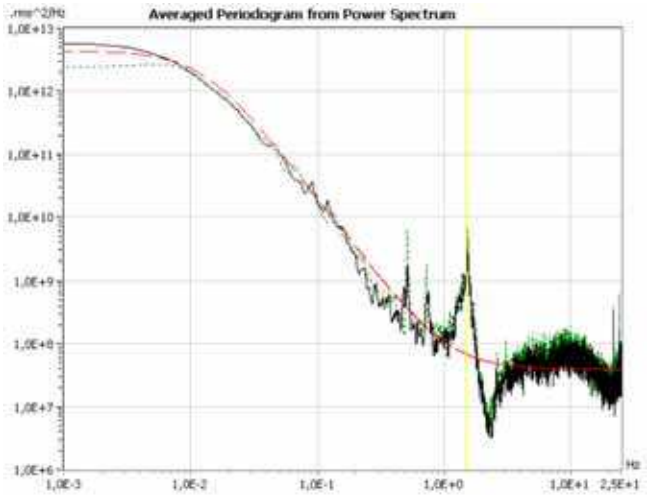

Fig. 13. $PSD_{Pfarm}^{+}(f)$ of a wind farm (in solid black) and $PSD_{Pturbine}^{+}(f)$ of one of its 648 kW turbines times 18 (in dashed green), for time series #1.

There is a peak in Fig. 14 at 2 Hz < f < 2,5 Hz. The analyzed turbine may have comparative less fluctuations in such range than the other turbines in the farm (the measured turbine may have better adjusted rotor and blades, while others turbines may suffer from more vibration effects). But other feasible reason is a higher correlation degree between the turbines at such frequency band, probably induced by turbine control or voltage variations.

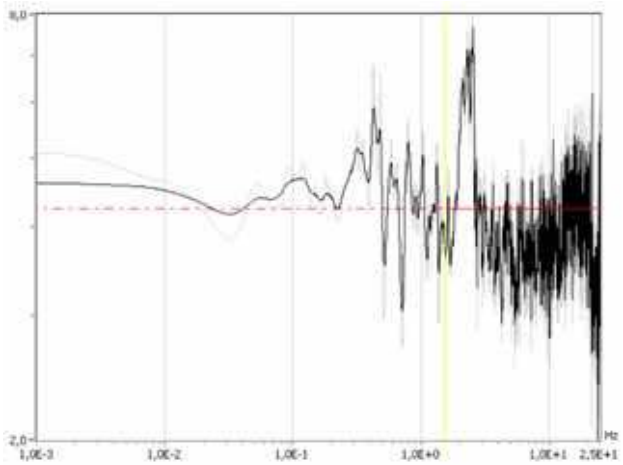

Fig. 14. Admittance of the active power (ratio of the farm *PSD* to the turbine *PSD)*.

In short, real power oscillations quicker than one minute can be considered independent among turbines of a wind farm because the *PSD* due to fast turbulence and rotational effects scales proportionally to the number of turbines.

The former section has analyzed values logged with high time resolution (each grid cycle, 20 ms) but the duration was relatively short (a bit more than 10 minutes) due to storage limitations in the recording system. Ten-minute records with 20 ms time resolution allow studying fluctuations with durations between some tenths of second up to one minute However, this duration is insufficient for analyzing wind farm dynamics slower than 0.016 Hz with acceptable uncertainty.

6. Case study: comparison of PSD of a wind farm with respect to one of its turbines during a day

In order to study the behaviour of fluctuations slower than one minute, the next section will analyze the mean power of each second during a day. Daily records with one second time resolution allow to study the fluctuations with durations from a few seconds up to an hour.
Overall, the transition frequency from uncorrelated to correlated fluctuations is mild and, in fact, the ratio $PSD_{farm}(f)/\ PSD_{turbine}(f)$ depends noticeably on atmospheric conditions and it varies from one wind farm to another. This is one of the reasons why the values of the coherence decay factors A_{long} and A_{lat} may vary twofold among different sources.
At higher frequencies, the control and generator technology influences greatly the smoothness of the power delivery. At low frequencies and under rated power, the variability is mainly due to the wind because any turbine tries to extract the maximum amount of power from the wind, regardless of their technology. During full power generation, the fluctuations have smaller amplitude and higher frequency.
The case presented in this section corresponds to low/ mid wind speed, since this range presents bigger fluctuations. The wind direction does not present big deviations during the day and the atmospheric conditions can be considered similar during all the day.
For clarity, the turbine and the farm is generating bellow rated power during all the day presented in this sections, without null, maximum power or unavailability periods. These operating conditions present quite different features, and each functioning mode should be treated differently. Moreover, some intermittent power delivery may occur during the transition from one operation condition to another, and this event should be treated as a transient. In fact, this chapter is limited to the analysis of continuous operation, without considering transitory events (such features can be better studied with other tools).

6.1 Daily spectrograms

The PSD in the *fraction-of-time* probability framework is the long term average of auto spectrum density and it characterizes the behaviour of stochastically stationary systems. The spectrogram shows the spectrum evolution and the stationarity of signals can be tested with it. Every spectrogram column can be thought as the power spectrum of a small signal sample. Therefore, the PSD in the classical stochastic framework is the ensemble average of the power spectrums. For stationary systems, the classical and the *fraction-of-time* approaches are equivalent.
The analysis has been performed using the spectrogram of the active power. The frequency band is between 0,5 Hz (fluctuations of 2 second of duration, corresponding to $8{,}4 \cdot 10^5$ cycles/ day) and 6 cycles/ day (fluctuations of 4 hours of duration).

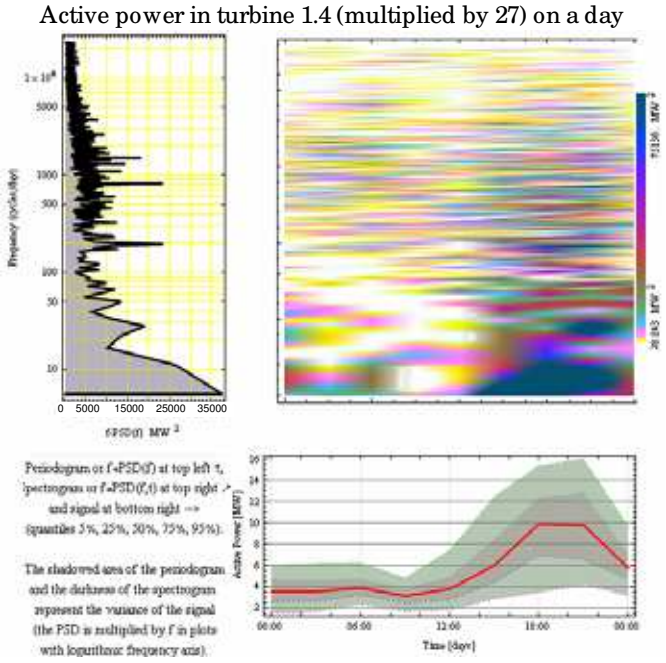

Fig. 15. Spectrogram of the real power [MW] at a turbine (times the turbines in the farm, 27).

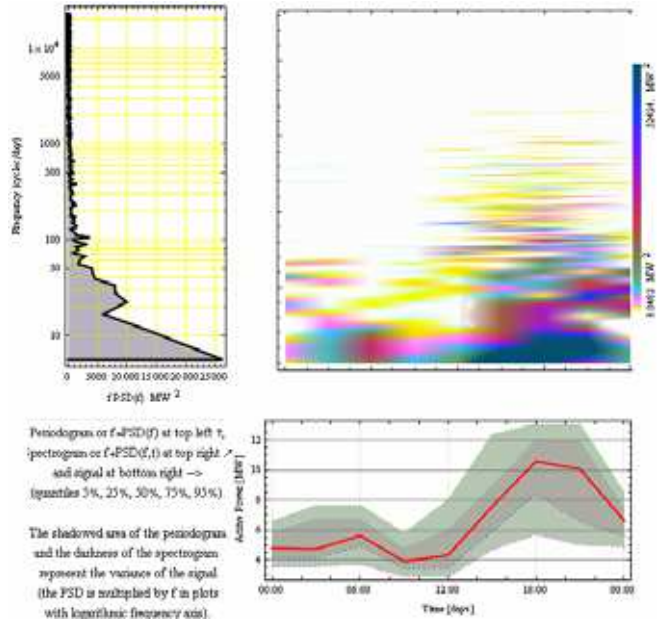

Fig. 16. Spectrogram of the real power [MW] at the substation.

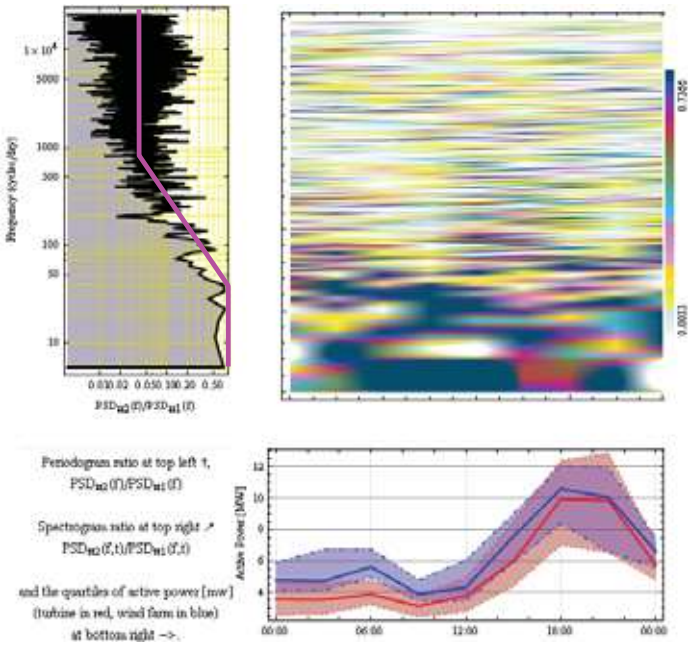

Fig. 17. Squared relative admittance $J^2(f)/N^2$ of the real power of the wind farm relative to the turbine computed as the spectrogram ratio.

	Module of coherence[f]	Appearance
Measured coherence	$\frac{\lvert SFFT_1[f,t]\,SFFT_2^*[f,t]\rvert}{\sqrt{PSD_1[f]\,PSD_2[f]}}$	thin, grey solid line
Fractional model	$\frac{5.58471}{5.58471+0.17906\,f^{0.621445}}$	thick, dotted red line
Power law model	$\frac{1.85021}{f^{0.294854}}$	dot–dashed blue line
Exponential model	$0.187372+0.760837\,e^{-0.00584543\,f}$	thin, dashed green line

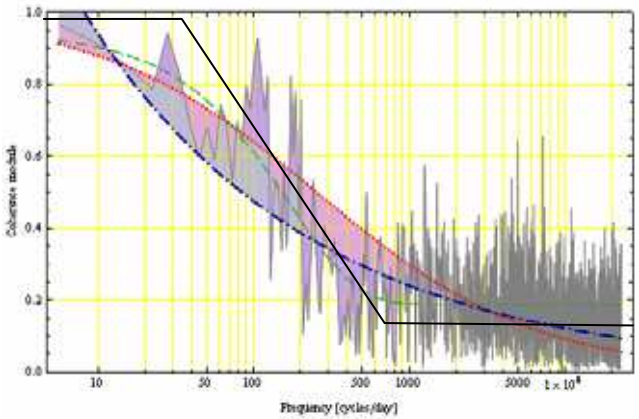

Fig. 18. Coherence models estimated by WINDFREDOM software.

Apart from the Short *FFT* (*SFFT*), the Wigner-Ville distribution (*WVD*) and the S-method (*SM*) have been tested to increase the frequency resolution of the spectrogram. However, the *SFFT* method has been found the most reliable since the amplitudes of the fluctuations are less distorted by the abundant cross-terms present in the power output (Boashash, 2003).

Fig. 15 and Fig. 16 show the spectrogram in the centre of the picture, codified by the scale shown on the right. The plots shown in this subsection have been produced with WINDFREDOM software, which is freely available (Mur-Amada, 2009). The regions with light colours (gray shades in the printed book) indicate that the power has a low content of fluctuations of frequencies corresponding to the vertical axis at the time corresponding to the horizontal axis. The zones with darker colours indicate that fluctuations of the frequency corresponding to the vertical axis have been noticeably observed at the time corresponding to the horizontal axis. For convenience, the median, the quartiles and the 5% and 95% quantiles of the wind speed are also shown in the bottom of the figures. The periodogram is shown on the left and it is computed by averaging the spectrogram.

Both the spectrogram and the periodogram show the auto-spectral density times frequency in Fig. 15 and Fig. 16, because the frequency scale is logarithmic (the derivative of the frequency logarithm is $1/f$). Therefore, the shadowed area of the periodogram or the darkness of the spectrogram is proportional to the variance of the power at each frequency.

Comparing Fig. 15 and Fig. 16, the fluctuations of frequencies higher than 40 cycles/ day are relatively smaller in the wind farm than in the turbine. The amount of smoothing at different frequencies is just the squared relative admittance $J^2(f)/N^2$ in Fig. 17. For convenience, $J^2(f)$ has been divided by the number of turbines because $J^2(f)/N^2 \sim 1$ for correlated fluctuations and $J^2(f)/N^2 \sim 1/N$ for uncorrelated fluctuations, (N = 27 is the number of turbines in the wind farm.

The wind farm admittance, corresponding to the periodogram and spectrogram of Fig. 16 divided by Fig. 15 is shown in Fig. 17. The magnitude scale is logarithmic in this plot to remark that the admittance reasonably fits a broken line in a double logarithmic scale.

In this farm, variations quicker than one and three-quarter of a minute (fluctuations of frequency larger than 800 cycles/ day) can be considered uncorrelated and fluctuations lasting more than 36 minutes (fluctuations of frequency smaller than 40 cycles/ day) can be considered fully correlated. In the intermediate frequency band, the admittance decays as a first order filter, in agreement with the spatial smoothing model.

Fig. 17 shows that the turbine and the wind farm medians (red and blue thick lines in the bottom plot) are similar because slow fluctuations affect both systems alike. The interquartil range (red and blue shadowed areas) is a bit larger in the scaled turbine power with respect to the wind farm. The range has the same magnitude order because the daily variance is primarily due to the correlated fluctuations, since the frequency content of the variance is concentrated in frequencies lower than 40 cycles/ day (see grey shadowed area in the periodograms on the left of Fig. 15 and Fig. 16).

In practice, the oscillations measured in the turbine are seen, to some extent, in the substation with some delay or in advance. The coherence $\vec{\gamma}_{\#1,\#2}$ is a complex magnitude with modulus between 0 and 1 and a phase, which represent the delay (positive angles) or the advance (negative angles) of the oscillations of the substation with respect to the turbine. Since the spectrum of a signal is complex, the argument of the coherence $\vec{\gamma}_{rc}(f)$ is the average phase difference of the fluctuations.

The coherence $\vec{\gamma}_{rc}(f)$ in Fig. 18 indicates the correlation degree and the time pattern of the fluctuations. The modulus is analogous to the correlation coefficient of the spectrum lines from both locations. If the ratio among complex power spectrums is constant (both in modulus and phase), then the coherence is the unity and its argument is the average phase difference. If the complex ratio is random (in modulus or phase), then the coherence is null. The uncertainty of the coherence can be decreased smoothing the plot in Fig. 18. The black broken line is the asymptotic approximation proposed in this chapter and the dashed and dotted lines correspond to other mathematical fits of the coherence.

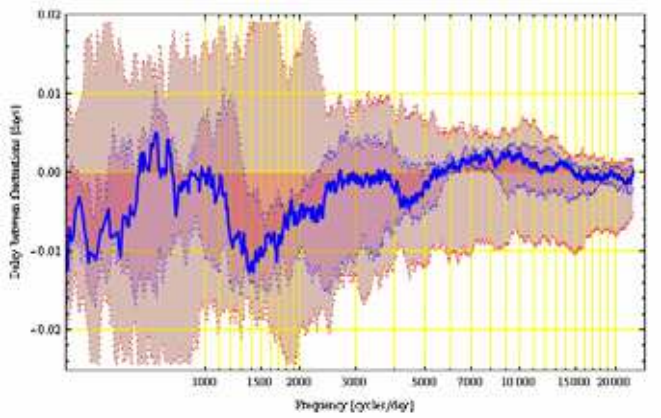

Fig. 19. Time delay quantiles between the fluctuation delays estimated by WINDFREDOM software.

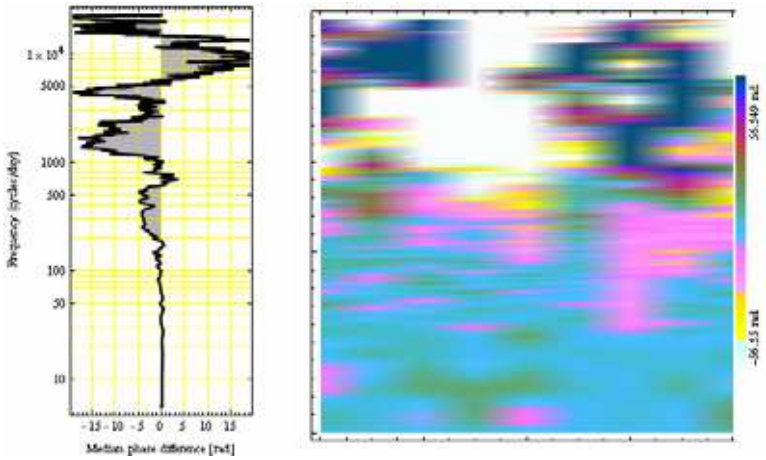

Fig. 20. Estimated phase delay between the power oscillations at the turbine and at the wind farm output. The median value for each frequency *f* is presented on the left and the phase differences of the spectrograms in Fig. 15 and Fig. 16 are presented on the right. A phase unwrapping algorithm has been used to reconstruct the phase from the *SFFT*.

The shadowed area in Fig. 19 indicates the 5%, 25%, 50%, 75% and 95% quantiles of the time delay τ between the oscillations observed at the turbine and the farm output. Fig. 19 shows that the time delay is less than half an hour (0.02 days) the 90% of the time. However, the time delay experiences great variability due to the stochastic nature of turbulence.

Wind direction is not considered in this study because it was steady during the data presented in the chapter. However, the wind direction and the position of the reference turbine inside the farm affect the time delay τ between oscillations. If wind direction changes, the phase difference, $\Delta\varphi = 2\pi f \tau$, can change notably in the transition frequency band, leading to very low coherences in that band. In such cases, data should be divided into series with similar atmospheric properties.

At frequencies lower than 40 cycles/ day, the time delays in Fig. 19 implies small phase differences, $\Delta\varphi = 2\pi f \tau$ (colorized in light cyan in Fig. 20), and fluctuations sum almost fully correlated. At frequencies higher than 800 cycles/ day, the phase difference $\Delta\varphi = 2\pi f \tau$ usually exceeds several times $\pm 2\pi$ radians (colorized in dark blue or white in Fig. 20), and fluctuations sum almost fully uncorrelated. It should be noticed that the phase difference $\Delta\varphi$ exceeds several revolutions at frequencies higher than 3000 cycles/ day and the estimated time delay in Fig. 10 has larger uncertainty (Ghiglia & Pritt, 1998). Thus, the unwrapping phase method could cause the time delay to be smaller at higher frequencies in Fig. 11.

This methodology has been used in (Mur-Amada & Bayod-Rujula, 2010) to compare the wind variations at several weather stations (wind speed behaves more linearly than generated power). The WINDFREDOM software is free and it can be downloaded from www.windygrid.org.

7. Conclusions

This chapter presents some data examples to illustrate a stochastic model that can be used to estimate the smoothing effect of the spatial diversity of the wind across a wind farm on the total generated power. The models developed in this chapter are based in the personal experience gained designing and installing multipurpose data loggers for wind turbines, and wind farms, and analyzing their time series.

Due to turbulence, vibration and control issues, the power injected in the grid has a stochastic nature. There are many specific characteristics that impact notably the power fluctuations between the first tower frequency (usually some tenths of Hertzs) and the grid frequency. The realistic reproduction of power fluctuations needs a comprehensive model of each turbine, which is usually confidential and private. Thus, it is easier to measure the fluctuations in a site and estimate the behaviour in other wind farms.

Variations during the continuous operation of turbines are experimentally characterized for timescales in the range of minutes to fractions of seconds. A stochastic model is derived in the frequency domain to link the overall behaviour of a large number of wind turbines from the operation of a single turbine. Some experimental measurements in the joint time-frequency domain are presented to test the mathematical model of the fluctuations.

The admittance of the wind farm is defined as the ratio of the oscillations from a wind farm to the fluctuations from a single turbine, representative of the operation of the turbines in the farm. The partial cancellation of power fluctuations in a wind farm are estimated from the ratio of the farm fluctuation relative to the fluctuation of one representative turbine.

Provided the Gaussian approximation is accurate enough, the wind farm power variability is fully characterized by its auto spectrum and many interesting properties can be estimated applying the outstanding properties of Gaussian processes (the mean power fluctuation shape during a period, the distribution of power variation in a time period, the most extreme power variation expected during a short period, etc.).

8. References

Abdi A.; Hashemi, H. & Nader-Esfahani, S. (2000). "On the PDF of the Sum of Random Vectors", IEEE Trans. on Communications. Vol. 48, No.1, January 2000, pp 7-12.

Alouini, M.-S.; Abdi, A. & Kaveh, M. (2001). "Sum of Gamma Variates and Performance of Wireless Communication Systems Over Nakagami-Fading Channels", IEEE Trans. On Vehicular Technology, Vol. 50, No. 6, (2001) pp. 1471-1480.

Amarís, H. & Usaola J. (1997). Evaluación en el dominio de la frecuencia de las fluctuaciones de tensión producidas por los generadores eólicos. V Jornadas Hispano-Lusas de Ingeniería Eléctrica. 1997.

Apt, J. (2007) "The spectrum of power from wind turbines", Journal of Power Sources 169 (2007) 369–374

Y. Baghzouz, R. F. Burch et alter (2002) "Time-Varying Harmonics: Part II—Harmonic Summation and Propagation", IEEE Trans. On Power Systems, Vol. 17, No. 1 (January 2002), pp. 279-285.

Bianchi, F. D.; De Battista, H. & Mantz, R. J. (2006). "Wind Turbine Control Systems. Principles, Modelling and Gain Scheduling Design", Springer, 2006.

Bierbooms, W.A.A.M. (2009) "Constrained Stochastic Simulation Of Wind Gusts For Wind Turbine Design", DUWIND Delft University Wind Energy Research Institute, March 2009.

Boashash, B. (2003). "Time Frequency, Signal Analysis and Processing. A comprehensive Reference". Ed. Elsevier, 2003.

Cavers, J.K. (2003). "*Mobile Channel Characteristics*", 2nd ed., Shady Island Press, 2003.

Cidrás, J.; Feijóo, A.E.; González C. C., (2002). "Synchronization of Asynchronous Wind Turbines" IEEE Trans, on Energy Conv., Vol. 17, No 4 (Nov. 2002), pp. 1162-1169

Comech-Moreno, M.P. (2007). "Análisis y ensayo de sistemas eólicos ante huecos de tension", Ph.D. Thesis, Zaragoza University, October 2007 (in Spanish).

Cushman-Roisin, B. (2007). "Environmental Fluid Mechanics", John Wiley & Sons, 2007.

Frandsen, S.; Jørgensen, H.E. & Sørensen, J.D. (2007) "Relevant criteria for testing the quality of turbulence models", 2007 European Wind Energy Conference and Exhibition, Milan (IT), 7-10 May 2007. pp. 128-132.

Gardner, W. A. (1994) "Cyclostationarity in Communications and Signal Processing", IEEE press, 1994.

Gardnera, W. A.; Napolitano, A. & Paurac, L. (2006) "Cyclostationarity: Half a century of research", Signal Processing 86 (April 2006), pp. 639–697.

Ghiglia, D.C. & Pritt, M.D. (1998). "Two-Dimensional Phase Unwrapping: Theory, Algorithms, and Software", John Whiley & Sons, 1998.

Hall, P.; & Heyde. C. C. (1980). Martingale Limit Theory and Its Application. New York: Academic Press (1980).

Kaimal, J.C. (1978). "Horizontal Velocity Spectra in an Unstable Surface Layer" Journal of the Atmospheric Sciences, Vol. 35, Issue 1 (January 1978), pp. 18–24.

Karaki, S. H. ; Salim B. A. & Chedid R. B. (2002). "Probabilistic Model of a Two-Site Wind Energy Conversion System", IEEE Transactions On Energy Conversion, Vol. 17, No. 4, December 2002.

Kundur, P. P.; Balu, N. J.; Lauby, M. G. (1994). "Power System Stability and Control", McGraw-Hill, 1994.

Li, P.; Banakar, H.; Keung, P. K.; Far H.G. & Ooi B.T. (2007). "Macromodel of Spatial Smoothing in Wind Farms", IEEE Trans, on Energy Conv., Vol. 22, No 1 (March. 2007), pp 119-128.

Martins, A.; Costa, P.C. & Carvalho, A. S. (2006). "Coherence And Wakes In Wind Models For Electromechanical And Power Systems Standard Simulations", European Wind Energy Conferences (EWEC 2006), February (2006), Athens.

Mur-Amada, J. (2009) "Wind Power Variability in the Grid", PhD. Thesis, Zaragoza University, October 2009. Available at www.windygrid.org

Mur-Amada, J. & Comech-Moreno, M.P. (2006). "Reactive Power Injection Strategies for Wind Energy Regarding its Statistical Nature", Sixth International Workshop on Large-Scale Integration of Wind Power and Transmission Networks for Offshore Wind Farm. Delft, October 2006.

Mur-Amada, J. & Bayod-Rújula, A.A. (2007). "Characterization of Spectral Density of Wind Farm Power Output", *9th Conference on Electrical Power Quality and Utilisation (EPQU'2007)*, Barcelona, October 2007.

Mur-Amada, J. & Bayod-Rújula, A.A. (2010). "Variability of Wind and Wind Power", *Wind Power*, Intech, Croatia, 2010. Available at: www.sciyo.com.

Norgaard, P. & Holttinen, H. (2004). "A Multi-turbine Power Curve Approach", in Proc. 2004 Nordic Wind Power Conference (NWPC 2002), Gothenberg, March 2004.

Press, W. H.; Teukolsky, S. A.; Vetterling, W. T. & Flannery, B. P. (2007). "Numerical Recipes. The Art of Scientific Computing", 3rd edition, Cambridge University Press, 2007.

Sanz M.; Llombart A.; Bayod A. A. & Mur, J. (2000) "Power quality measurements and analysis for wind turbines", *IEEE Instrumentation and Measurement Technical Conference 2000*, pp. 1167-1172. May 2000, Baltimore.

Saranyasoontorn, K.; Manuel, L. & Veers, P. S. "A Comparison of Standard Coherence Models form Inflow Turbulence With Estimates from Field Measurements", Journal of Solar Energy Engineering, Vol. 126 (2004), Issue 4, pp. 1069-1082

Schlez, W. & Infield, D. (1998). "Horizontal, two point coherence for separations greater than the measurement height", *Boundary-Layer Meteorology* 87 (1998), 459-480.

Schwab, M.; Noll, P. & Sikora, T. (2006). "Noise robust relative transfer function estimation", XIV European Signal Processing Conference, September 4 - 8, 2006, Florence, Italy.

Soens, J. (2005). "Impact Of Wind Energy In A Future Power Grid", Ph.D. Dissertation, Katholieke Universiteit Leuven, December 2005.

Sorensen, P.; Hansen, A. D. & Rosas C. (2002). "Wind models for simulation of power fluctuations from wind farms", Journal of Wind Engineering and Ind. Aerodynamics 90 (2002), pp. 1381-1402

Sørensen, P.; Cutululis, N. A.; Vigueras-Rodríguez, A; Madsen, H.; Pinson, P; Jensen, L. E.; Hjerrild, J. & Donovan M., (2008) "Modelling of Power Fluctuations from Large Offshore Wind Farms", *Wind Energy*,Volume 11, Issue 1, pages 29–43, January/ February 2008.

Stefopoulos, G.; Meliopoulos A. P.& Cokkinides G. J. (2005), "Advanced Probabilistic Power Flow Methodology", 15th PSCC, Liege, 22-26 August 2005

Su, C-L. (2005) "Probabilistic Load-Flow Computation Using Point Estimate Method", IEEE Trans. Power Systems, Vol. 20, No. 4, November 2005, pp. 1843-1851.

Tentzerakis, S. T. & Papathanassiou S. A. (2007), "An Investigation of the Harmonic Emissions of Wind Turbines", IEEE Trans, on Energy Conv., Vol. 22, No 1, March. 2007, pp 150-158.

Thiringer, T.; Petru, T.; & Lundberg, S. (2004) "Flicker Contribution From Wind Turbine Installations" IEEE Trans, on Energy Conv., Vol. 19, No 1, March 2004, pp 157-163.

Vilar Moreno, C. (2003). "Voltage fluctuation due to constant speed wind generators" Ph.D. Thesis, Carlos III University, Leganés, Spain, 2003.

Wangdee, W. & Billinton R. (2006). "Considering Load-Carrying Capability and Wind Speed Correlation of WECS in Generation Adequacy Assessment", IEEE Trans, on Energy Conv., Vol. 21, No 3, September 2006, pp. 734-741.

Welfonder, E.; Neifer R. & Spaimer, M. (1997) "Development And Experimental Identification Of Dynamic Models For Wind Turbines", Control Eng. Practice, Vol. 5, No. 1 (January 2007), pp. 63-73.

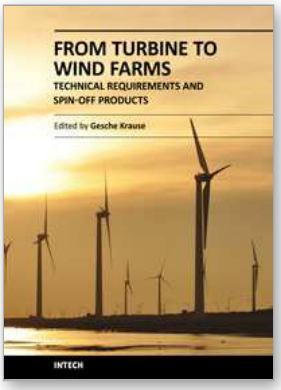

From Turbine to Wind Farms - Technical Requirements and Spin-Off Products

Edited by Dr. Gesche Krause

ISBN 978-953-307-237-1
Hard cover, 218 pages
Publisher InTech
Published online 04, April, 2011
Published in print edition April, 2011

This book is a timely compilation of the different aspects of wind energy power systems. It combines several scientific disciplines to cover the multi-dimensional aspects of this yet young emerging research field. It brings together findings from natural and social science and especially from the extensive field of numerical modelling.

How to reference

In order to correctly reference this scholarly work, feel free to copy and paste the following:

Joaquin Mur-Amada and Jesús Sallán-Arasanz (2011). Power Fluctuations in a Wind Farm Compared to a Single Turbine, From Turbine to Wind Farms - Technical Requirements and Spin-Off Products, Dr. Gesche Krause (Ed.), ISBN: 978-953-307-237-1, InTech, Available from: http://www.intechopen.com/books/from-turbine-to-wind-farms-technical-requirements-and-spin-off-products/power-fluctuations-in-a-wind-farm-compared-to-a-single-turbine

INTECH
open science | open minds

InTech Europe
University Campus STeP Ri
Slavka Krautzeka 83/A
51000 Rijeka, Croatia
Phone: +385 (51) 770 447
Fax: +385 (51) 686 166
www.intechopen.com

InTech China
Unit 405, Office Block, Hotel Equatorial Shanghai
No.65, Yan An Road (West), Shanghai, 200040, China
中国上海市延安西路65号上海国际贵都大饭店办公楼405单元
Phone: +86-21-62489820
Fax: +86-21-62489821